Design of a Maximum Power Tracking System for Wind-Energy-Conversion Applications

Eftichios Koutroulis and Kostas Kalaitzakis

Abstract—**A wind-generator (WG) maximum-power-point-tracking (MPPT) system is presented, consisting of a high-efficiency buck-type dc/dc converter and a microcontroller-based control unit running the MPPT function. The advantages of the proposed MPPT method are that no knowledge of the WG optimal power characteristic or measurement of the wind speed is required and the WG operates at a variable speed. Thus, the system features higher reliability, lower complexity and cost, and less mechanical stress of the WG.**

Experimental results of the proposed system indicate near-optimal WG output power, increased by 11%–50% compared to a WG directly connected via a rectifier to the battery bank. Thus, better exploitation of the available wind energy is achieved, especially under low wind speeds.

Index Terms—**Buck converter, maximum power point tracking (MPPT), microcontroller, variable speed, wind generator (WG).**

I. Introduction

WIND GENERATORS (WGs) have been widely used both in autonomous systems for power supplying remote loads and in grid-connected applications. Although WGs have a lower installation cost compared to photovoltaics, the overall system cost can be further reduced using high-efficiency power converters, controlled such that the optimal power is acquired according to the current atmospheric conditions.

The WG power production can be mechanically controlled by changing the blade pitch angle [1]. However, WGs of special construction are required, which is not the usual case, especially in small-size stand-alone WG systems.

A commonly used WG control system [2]–[4] is shown in Fig. 1(a). This topology is based on the WG optimal power versus the rotating-speed characteristic, which is usually stored in a microcontroller memory. The WG rotating speed is measured; then, the optimal output power is calculated and compared to the actual WG output power. The resulting error is used to control a power interface. In a similar version found in [5], the WG output power is measured and the target rotor speed for optimal power generation is derived from the WG optimal power versus rotor-speed characteristic. The target rotor speed is compared to the actual speed, and the error is used to control a dc/dc power converter. The control algorithm has been implemented in LabVIEW running on a PC.

Manuscript received February 26, 2003; revised May 30, 2004. Abstract published on the Internet January 25, 2006.

The authors are with the Department of Electronic and Computer Engineering, Technical University of Crete, Chania GR-73100, Greece (e-mail: koskal@electronics.tuc.gr).

Digital Object Identifier 10.1109/TIE.2006.870658

In permanent-magnet (PM) WG systems, the output current and voltage are proportional to the electromagnetic torque and rotor speed, respectively. In [6] and [7], the rotor speed is calculated according to the measured WG output voltage, while the optimal output current is calculated using an approximation of the current versus the rotational-speed optimal characteristic. The error resulting from the comparison of the calculated and the actual current is used to control a dc/dc converter.

The disadvantage of all above methods is that they are based on the knowledge of the WG optimal power characteristic, which is usually not available with a high degree of accuracy and also changes with rotor aging. Another approach using a two-layer neural network [8] updates online the preprogrammed WG power characteristic by perturbation of the control signals around the values provided by the power characteristic. However, under real operating conditions where the wind speed changes rapidly, the continuous neural-network training required results in accuracy and control-speed reduction.

A control system based on wind-speed measurements [2] is shown in Fig. 1(b). The wind speed is measured, and the required rotor speed for maximum power generation is computed. The rotor speed is also measured and compared to the calculated optimal rotor speed, while the resulting error is used to control a power interface.

Implementations of fuzzy-logic-based control systems transferring the maximum power from a wind-energy-conversion system to the utility grid or to a stand-alone system have been presented in [9] and [10], respectively. The controllers are based on a polynomial approximation of the optimal power versus the wind-speed characteristic of the WG.

Apart from the accuracy reduction due to the approximation of the WG characteristics, an accurate anemometer is required for the implementation of the aforementioned methods, which increases the system cost. Furthermore, due to wind gusts of low-energy profile, extra processing of wind-speed measurement must be incorporated in the control system for a reliable computation of the available wind energy, which increases the control system complexity.

In this paper, an alternative approach for WG maximum-power-point-tracking (MPPT) control is described. The block diagram of the proposed system is illustrated in Fig. 2. The MPPT process is based on monitoring the WG output power using measurements of the WG output voltage and current and directly adjusting the dc/dc converter duty cycle according to the result of comparison between successive WG-output-power values. Thus, neither knowledge of the WG power

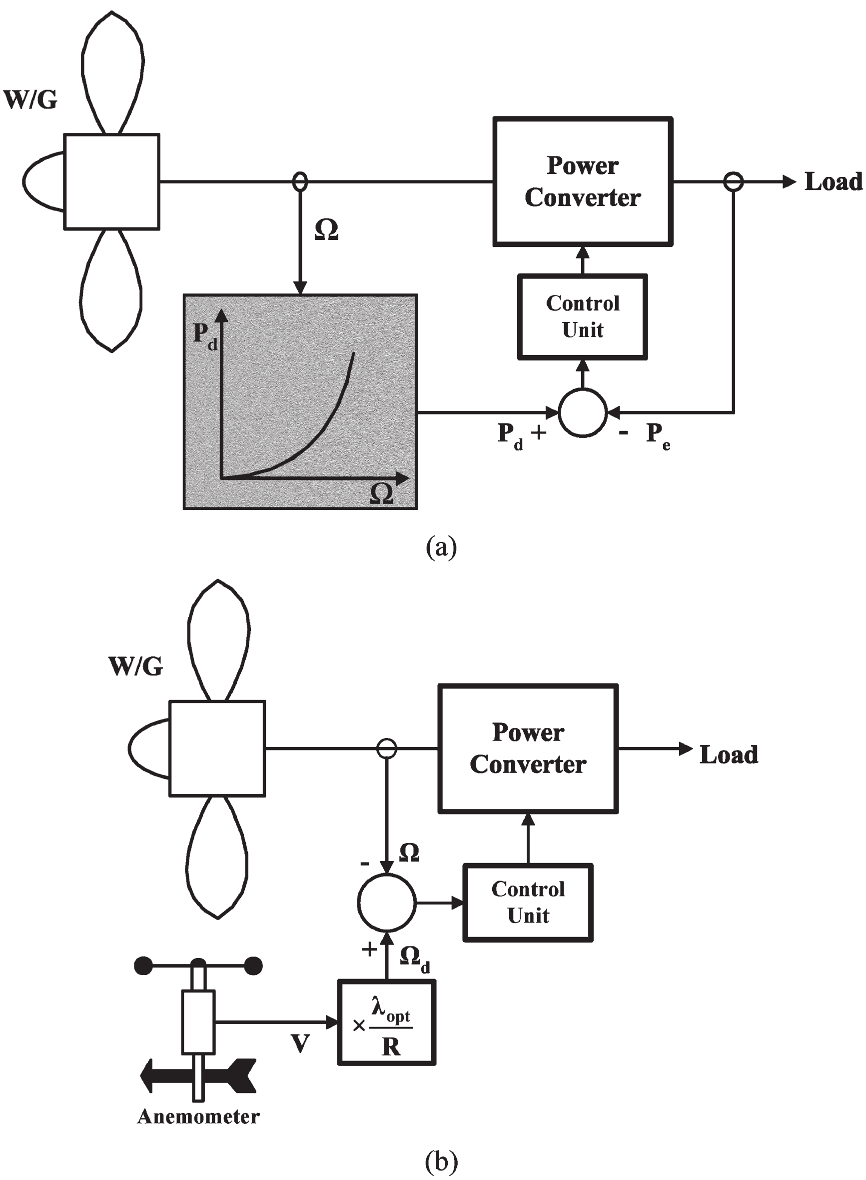

Fig. 1. WG MPPT methods. (a) Control system based on rotating-speed measurements. (b) Control system based on wind-speed measurements.

versus the rotor speed of rotation or wind-speed characteristic nor measurements of the wind speed are required. A resistive dummy load is used to protect the WG from over-speeding. The proposed MPPT method does not depend on the WG wind and rotor-speed ratings or the dc/dc converter power rating. Although the proposed method has been tested on a battery-charging application using a dc/dc converter, it can also be extended in grid-connected applications by appropriate modification of the dc/ac inverter control. The proposed system is built around a high-efficiency dc/dc converter and a low-cost microcontroller unit, which can easily perform additional operations such as battery charging management and/or control of additional renewable energy sources (RES).

This paper is organized as follows. The WG characteristics are described in Section II, the proposed system is analyzed in Section III, and the theoretical and experimental results are presented in Section IV.

II. WG Characteristics

The power captured by the WG blades P_{m} is a function of the blade shape, the pitch angle, and the radius and the rotor speed of rotation

$$P_{\mathrm{m}} = \frac{1}{2}\pi\rho C_{\mathrm{p}}(\lambda,\beta)R^2V^3 \tag{1}$$

where ρ is the air density (typically 1.25 kg/m^3), β is the pitch angle (in degrees), $C_{\mathrm{p}}(\lambda,\beta)$ is the wind-turbine power coefficient, R is the blade radius (in meters), and V is the wind speed (in m/s). The term λ is the tip-speed ratio, defined as

$$\lambda = \frac{\Omega R}{V} \tag{2}$$

where Ω is the WG rotor speed of rotation (rad/s).

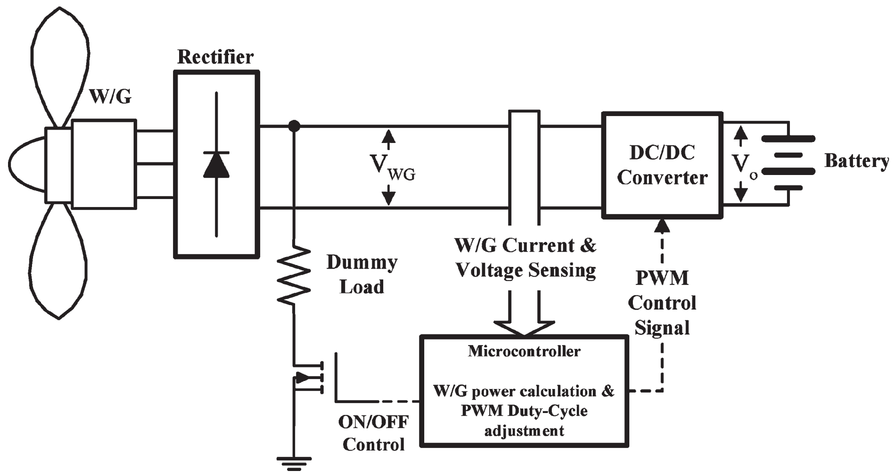

Fig. 2. Block diagram of the proposed system.

Considering the generator efficiency η_{G}, the total power produced by the WG P is

$$P = \eta_{\mathrm{G}} P_{\mathrm{m}}. \tag{3}$$

The WG power coefficient is maximized for a tip-speed ratio value λ_{opt} when the blades pitch angle is $\beta = 0°$. The WG power curves for various wind speeds are shown in Fig. 3. It is observed that, for each wind speed, there exists a specific point in the WG output power versus rotating-speed characteristic where the output power is maximized. The control of the WG load results in a variable-speed WG operation, such that maximum power is extracted continuously from the wind (MPPT control). The value of the tip-speed ratio is constant for all maximum power points (MPPs), while the WG speed of rotation is related to the wind speed as follows:

$$\Omega_{\mathrm{n}} = \lambda_{\mathrm{opt}} \frac{V_{\mathrm{n}}}{R} \tag{4}$$

where Ω_{n} is the optimal WG speed of rotation at a wind velocity V_{n}.

Besides the optimal energy production capability, another advantage of variable-speed operation is the reduction of stress on the WG shafts and gears, since the blades absorb the wind torque peaks during the changes of the WG speed of rotation. The disadvantage of variable-speed operation is that a power conditioner must be employed to play the role of the WG apparent load. However, the evolution of power electronics helps reduce the power-converter cost and increase its reliability, while the higher cost is balanced by the energy production gain.

The torque curves of the WG, consisting of the interconnected wind-turbine/generator system, for various generator output voltage levels under various wind speeds, are shown in Fig. 4. The generator is designed such that it operates in the approximately linear region corresponding to the straight portion of the generator torque curves in Fig. 4, under any wind-speed condition. The intersection of the generator torque curve with the wind-turbine torque curve determines the WG operating point. During the MPPT process, a change of the WG apparent load results in variable generator output voltage level; thus, the generator torque is adjusted such that the generator operates at the target torque (e.g., point A) under any wind speed. The target-torque line corresponds to the optimal-power-production line indicated in Fig. 3, where the energy extracted from the WG system is maximized.

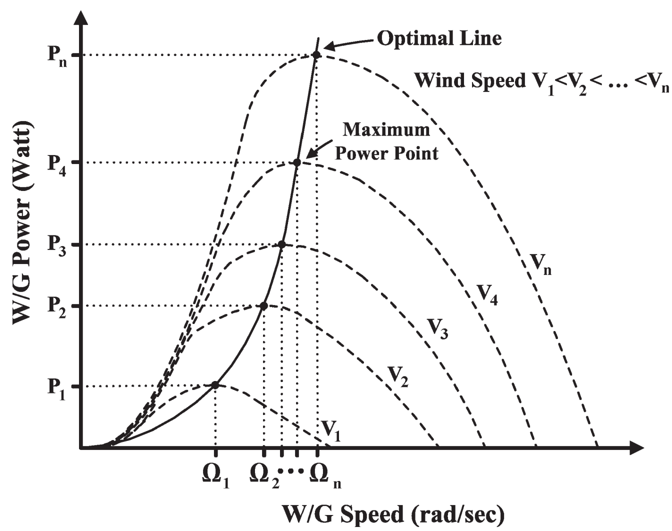

Fig. 3. WG power curves at various wind speeds.

III. Proposed System

A. MPPT Algorithm

As mentioned in Section I, the MPPT process in the proposed system is based on directly adjusting the dc/dc converter duty cycle according to the result of the comparison of successive WG-output-power measurements. Although the wind speed varies highly with time, the power absorbed by the WG varies relatively slowly, because of the slow dynamic response of the interconnected wind-turbine/generator system. Thus, the problem of maximizing the WG output power using the converter duty cycle as a control variable can be effectively solved using the steepest ascent method according to the following control law:

$$D_k = D_{k-1} + C_1 \cdot \frac{\Delta P_{k-1}}{\Delta D_{k-1}} \tag{5}$$

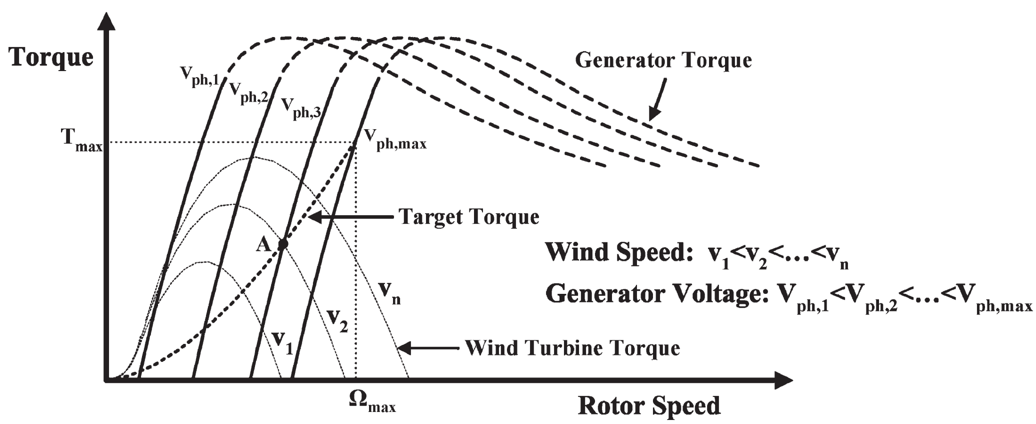

Fig. 4. Torque–speed characteristics of the wind turbine and the generator.

where D_k and D_{k-1} are the duty-cycle values at iterations k and $k-1$, respectively $(0 < D_k < 1)$; $\Delta P_{k-1}/\Delta D_{k-1}$ is the WG power gradient at step $k-1$; and C_1 is the step change.

In order to ensure that this method results in convergence to the WG MPP at any wind-speed level, it is adequate to prove that the function $P(D)$, relating the WG power P and the dc/dc converter duty cycle D, has a single extreme point coinciding with the WG MPPs depicted in Fig. 3.

Considering the WG power characteristics depicted in Fig. 3, it is obvious that at the points of maximum power production

$$\frac{dP}{d\Omega} = 0 \tag{6}$$

where Ω is the WG rotor speed.

Applying the chain rule, the above equation can be written as

$$\frac{dP}{d\Omega} = \frac{dP}{dD} \cdot \frac{dD}{dV_{\mathrm{WG}}} \cdot \frac{dV_{\mathrm{WG}}}{d\Omega_{\mathrm{e}}} \cdot \frac{d\Omega_{\mathrm{e}}}{d\Omega} = 0 \tag{7}$$

where V_{WG} is the rectifier output voltage level and Ω_{e} is the generator-phase-voltage angular speed.

In case of a buck-type dc/dc converter, its input voltage is related to the output (battery) voltage and the duty cycle as follows:

$$D = \frac{V_{\mathrm{o}}}{V_{\mathrm{WG}}}$$
$$\frac{dD}{dV_{\mathrm{WG}}} = -\frac{1}{V_{\mathrm{WG}}^2} V_{\mathrm{o}} \neq 0 \tag{8}$$

where V_{o} is the battery voltage level.

The wind-turbine rotor speed is related to the generator speed as follows:

$$\Omega_{\mathrm{e}} = p \cdot \Omega$$
$$\frac{d\Omega_{\mathrm{e}}}{d\Omega} = p > 0 \tag{9}$$

where p is the generator number of pole pairs.

The rectifier output voltage V_{WG} is proportional to the generator phase voltage V_{ph}; considering Fig. 4, it is concluded that

$$\frac{dV_{\mathrm{ph}}}{d\Omega_{\mathrm{e}}} > 0 \tag{10}$$

and

$$\frac{dV_{\mathrm{WG}}}{d\Omega_{\mathrm{e}}} > 0. \tag{11}$$

Considering (7)–(11), it holds that

$$\frac{dP}{d\Omega} = 0 \quad \Leftrightarrow \quad \frac{dP}{dD} = 0. \tag{12}$$

Thus, the function $P(D)$ has a single extreme point, coinciding with the WG MPP, and the dc/dc converter duty-cycle adjustment according to the control law of (5) ensures convergence to the WG MPP under any wind-speed condition.

The power maximization process is shown in Fig. 5. Since the duty-cycle adjustment follows the direction of dP/dD, the duty-cycle value is increased in the high-speed side of the WG characteristic, resulting in a WG-rotor-speed reduction and power increase, until the MPP is reached. Similarly when the starting point is in the low-speed side, following the direction of dP/dD results in duty-cycle reduction and the subsequent convergence at the MPP, since the WG rotor speed is progressively increased.

The proposed method can also be applied to maximize the output power of the WG in case of alternative dc/dc converter configurations.

1) Boost converter: $V_{\mathrm{WG}} = (1-D)V_{\mathrm{o}}$, $dV_{\mathrm{WG}}/dD = -V_{\mathrm{o}} \neq 0$.
2) Buck–boost converter: $V_{\mathrm{WG}} = V_{\mathrm{o}}(1-D)/D$, $dV_{\mathrm{WG}}/dD = -(1/D^2)V_{\mathrm{o}} \neq 0$.
3) Cuk converter: $V_{\mathrm{WG}} = V_{\mathrm{o}}(1-D)/D$, $dV_{\mathrm{WG}}/dD = -(1/D^2)V_{\mathrm{o}} \neq 0$.
4) Flyback converter: $V_{\mathrm{WG}} = V_{\mathrm{o}}(1-D)/D$, $dV_{\mathrm{WG}}/dD = -(1/D^2)V_{\mathrm{o}} \neq 0$.

In order to reduce the impact of the sensor accuracy on the generated power, the control law of (5) has been implemented

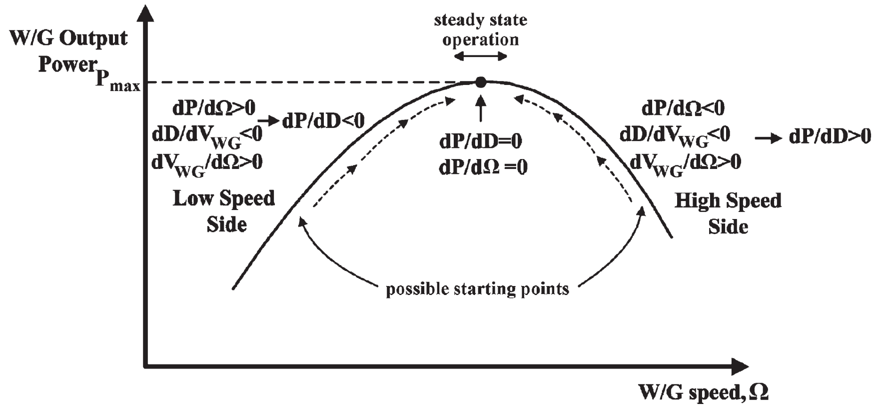

Fig. 5. MPP tracking process.

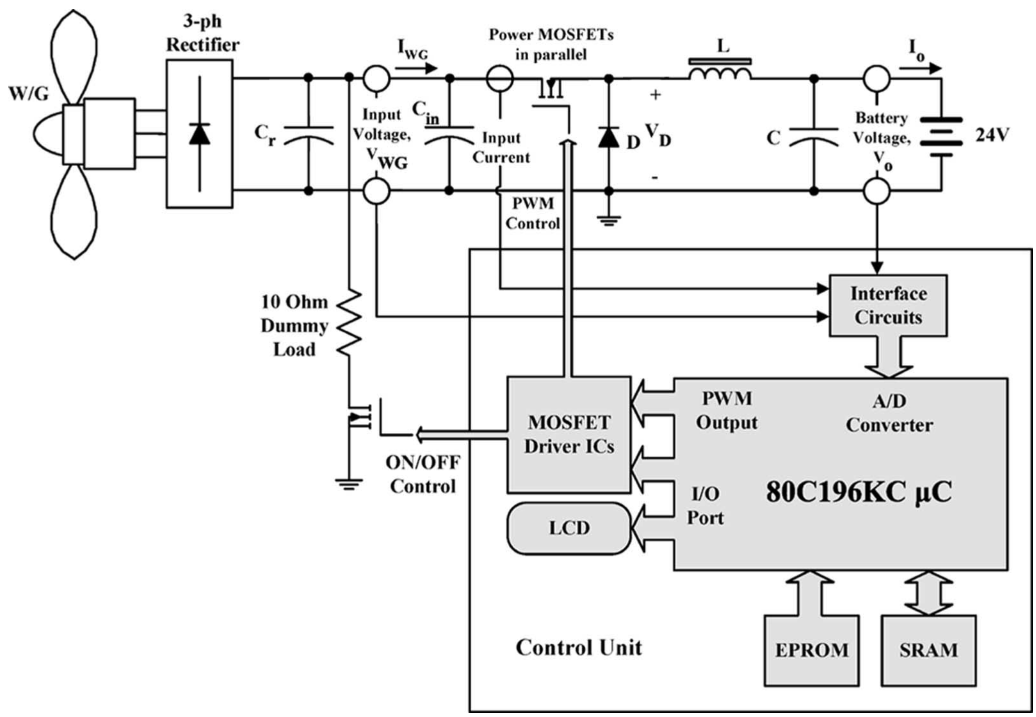

Fig. 6. Detailed diagram of the proposed system.

based on incremental WG power measurements, rather than absolute measurements, as follows:

$$\begin{aligned} D_k &= D_{k-1} + \Delta D_{k-1} \\ \Delta D_{k-1} &= C_2 \cdot \text{sign}(\Delta D_{k-2}) \cdot \text{sign}(P_{\text{in},k-1} - P_{\text{in},k-2}) \end{aligned} \quad (13)$$

where ΔD_{k-1} is the duty-cycle change at step $k-1$; $P_{\text{in},k-1}$ and $P_{\text{in},k-2}$ are the converter input-power levels at steps $k-1$ and $k-2$, respectively; C_2 is a constant determining the speed and accuracy of the convergence to the MPP; and the function $\text{sign}(x)$ is defined as

$$\begin{aligned} \text{sign}(x) &= 1, \qquad \text{if } x \geq 0 \\ \text{sign}(x) &= -1, \qquad \text{if } x < 0. \end{aligned} \quad (14)$$

B. Power-Electronic Interface

The detailed diagram of the proposed system is depicted in Fig. 6. The WG ac output voltage is first converted to dc form using a three-phase full-wave bridge rectifier. The rectifier output capacitor value C_{r} is calculated as follows:

$$C_r \geq \frac{1}{12fR_{\text{L}}}\left(1 + \frac{1}{\sqrt{2}\text{RF}}\right) \quad (15)$$

where R_{L} is the WG load resistance, f is the WG output voltage frequency, and RF is the rectifier output voltage ripple factor.

A buck-type dc/dc converter is used to convert the high dc input voltage to the 24-V battery voltage level. The flyback diode D is of fast-switching type, while four power MOSFETs are connected in parallel, to comply with the converter power capability requirements. A power MOSFET is used to switch on and off a 10-Ω resistive dummy load, thus limiting the WG speed of rotation under severe conditions.

The power inductor L and the input and output capacitor values, $C_{\rm in}$ and C, respectively, are calculated as follows [11]:

$$L \geq \frac{V_{\rm om}(1-D_{\rm cm})}{f_{\rm s}|\Delta I_{\rm Lm}|} \tag{16}$$

$$C \geq \frac{1}{8}\frac{(1-D_{\rm cm})}{{\rm L}f_{\rm s}^2{\rm RF_o}} \tag{17}$$

$$C_{\rm in} \geq \frac{(1-D_{\rm cm})I_{\rm om}D_{\rm cm}}{{\rm RF_{in}}V_{\rm WGm}f_{\rm s}} \tag{18}$$

where $f_{\rm s}$ is the dc/dc converter switching frequency, $D_{\rm cm}$ is the duty cycle at maximum output power of the converter, $\Delta I_{\rm Lm}$ is the peak-to-peak ripple of the inductor current, $V_{\rm om}$ is the maximum of the dc component of the output voltage, $I_{\rm om}$ is the dc component of the output current at maximum output power, $\rm RF_o$ is the output voltage ripple factor (typically $\rm RF_o \leq 2\%$), $\rm RF_{in}$ is the input voltage ripple factor (typically $\rm RF_{in} \leq 2\%$), and $V_{\rm WGm}$ is the converter input voltage at maximum power.

The control unit is supplied by the battery and consists of an Intel 80C196KC microcontroller unit with an external erasable programmable ROM (EPROM) and a static RAM (SRAM), the interface circuits comprising of sensors and amplifiers connected to the on-chip A/D converter, as well as the power MOSFET IC drivers. A 39.2-kHz 8-bit-resolution on-chip pulsewidth modulation (PWM) output is used to control the power MOSFETs of the buck converter through the IR2104 driver IC, while an I/O port pin controls the power MOSFET that switches the dummy load through the IR2121 driver IC. Another I/O port is used to drive a liquid crystal display (LCD) showing various parameters of the system operation.

The WG and battery voltages are measured by means of voltage dividers interfaced to operational-amplifier (op-amp)-based voltage-follower circuits. The dc/dc converter input current is equal to the average value of the power MOSFET current, which has a pulse-type waveform and is measured with a unidirectional current transformer.

The flowchart of the control algorithm is shown in Fig. 7. The battery voltage is monitored and when it reaches a predefined set point, the MPPT operation is suspended in order to protect the battery stack from overcharging.

The PWM duty-cycle value is stored in an 8-bit register of the microcontroller, taking values that correspond to duty-cycle values 0%–99.6%. The WG output power is calculated and compared to the WG output power at the previous iteration of the algorithm. According to the result of the comparison, the sign of the duty-cycle change ΔD is either complemented or remains unchanged. Subsequently, the PWM output duty cycle is changed appropriately, thus implementing the control law described by (13).

After the duty-cycle regulation, the WG voltage is checked; if it is higher than the maximum preset limit, the dummy load is connected to the dc/dc converter input in order to protect the WG from overspeeding. The dummy load is disconnected when the WG output voltage falls below the lower preset limit. The hysteresis introduced by the maximum and minimum preset limits is necessary to avoid the dummy load continuous on/off switching.

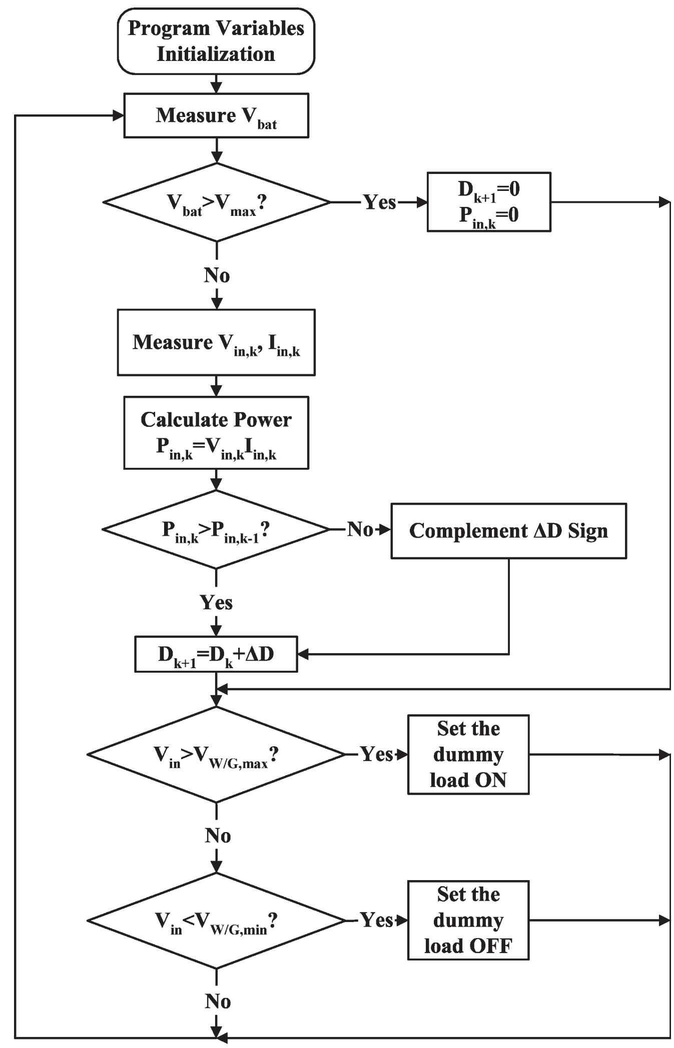

Fig. 7. MPPT process algorithm.

IV. Theoretical and Experimental Results

A prototype MPPT system was developed based on the method described above. The WG used in the experiments has a three-phase output rated at 100-V rms; thus, the dummy-load connection and disconnection voltage levels are set at 140 and 100 V, respectively.

The dc/dc converter was designed according to the methodology analyzed in Section III. The power switch consists of four MOSFETs rated at 200 V and 30 A each, while the flyback diode has a 200-ns reverse-recovery time. The calculated input and output capacitor values are 470 and 4700 μF, respectively. The output inductor value is 45 μH and is wound on a Siemens E65/21 ferrite core with a 3-mm air gap. The experimental waveform of the diode D voltage is depicted in Fig. 8. The converter operates in continuous conduction mode, and the

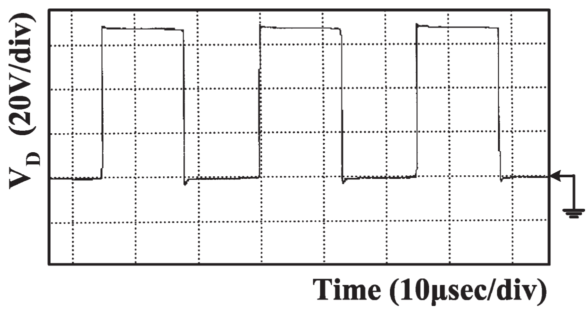

Fig. 8. Experimental waveform of the dc/dc converter diode D voltage, V_{D}.

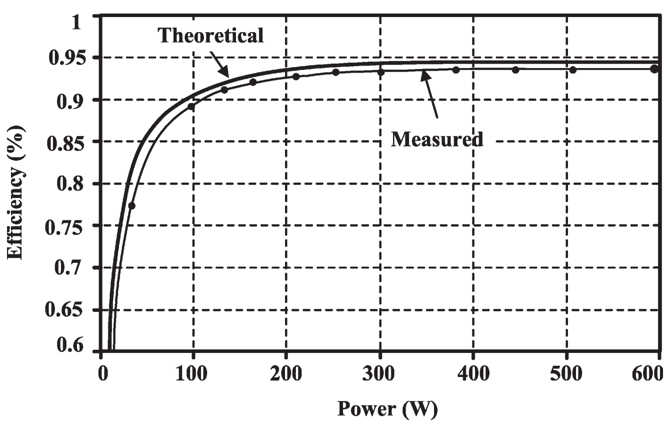

Fig. 9. DC/DC converter efficiency versus output power.

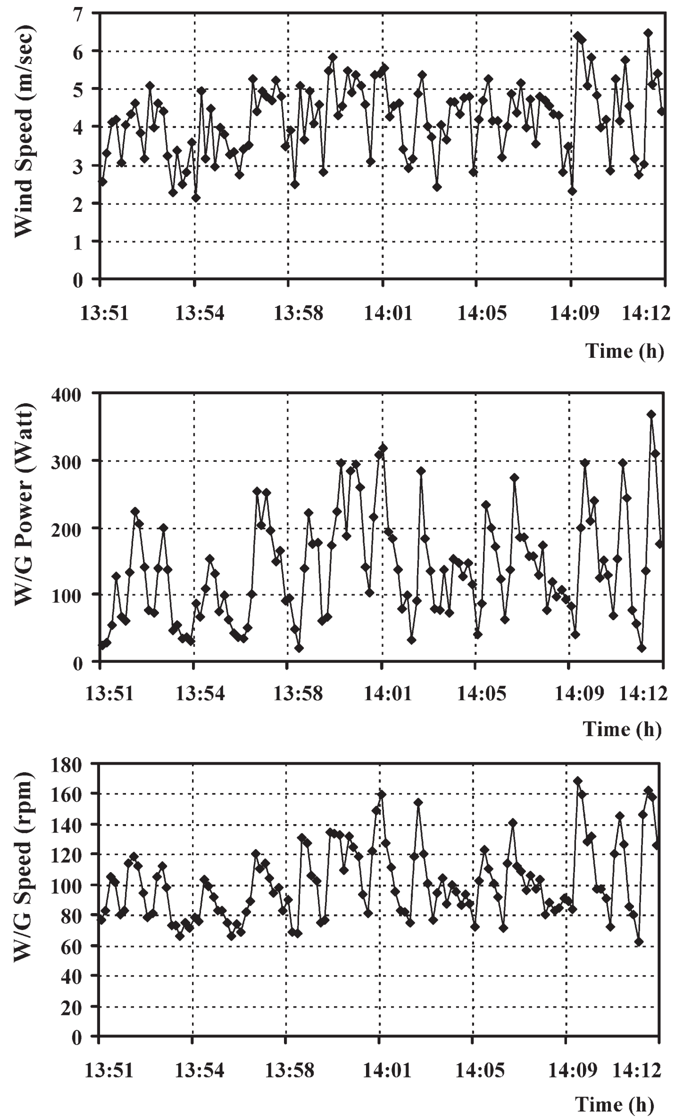

Fig. 10. Wind speed, WG output power, and WG rotational speed versus time.

switching frequency is approximately 40 kHz. The dc input voltage value in this case is $V_{\mathrm{WG}} = 66.8$ V, and the dc output voltage value is $V_{\mathrm{O}} = 33.9$ V. Such a high value of the output (battery) voltage appears in case that the battery is fully charged and a sudden increase of the converter input power follows. If this is the case, the MPPT process is suspended according to the MPPT algorithm flowchart shown in Fig. 7. The dc/dc converter efficiency is defined as

$$\eta = \frac{P_{\mathrm{o}}}{P_{\mathrm{in}}} = \frac{P_{\mathrm{o}}}{P_{\mathrm{o}} + P_{\mathrm{d}}} \tag{19}$$

where P_{in} and P_{o} are the dc/dc converter input and output power, respectively, and P_{d} is the power loss consisting of the MOSFET and diode conduction and switching losses, the inductor core and copper losses, and the control system power consumption.

The theoretical and measured efficiency for various output-power levels is shown in Fig. 9. The theoretical values were calculated using data given by the manufacturers of the circuit elements. It is observed that the efficiency is quite high and relatively constant for a wide output power range. This is important in WG systems since the generated power depends strongly on the atmospheric conditions and varies over a wide range. The wind speed, the WG output power, and the corresponding rotor speed of rotation, measured during a 22-min time period and sampled with a 0.1-Hz rate, are depicted in Fig. 10. It is observed that the WG power production follows the changes of the wind speed.

In order to further evaluate the MPPT performance, the wind speed, the WG power, and the WG rotational speed were measured during a 4-h test period with a 0.1-Hz sampling rate. The measured WG rotational-speed range was divided in intervals of 10-r/min width each, and the ensemble average (P_i, Ω_i) of the WG power and rotational-speed measurements corresponding to each interval was calculated as follows [2]:

$$P_i = \frac{1}{n_i} \sum_{j=1}^{n_i} P_{ij} \tag{20}$$

$$\Omega_i = \frac{1}{n_i} \sum_{j=1}^{n_i} \Omega_{ij} \tag{21}$$

where Ω_{ij} is the jth rotational-speed measurement in the ith interval, P_{ij} is the jth power measurement in the ith interval, and n_i is the number of data sets in the ith interval. The resulting ensemble averages (P_i, Ω_i) were used to build the diagram shown in Fig. 11. It can be concluded that, using

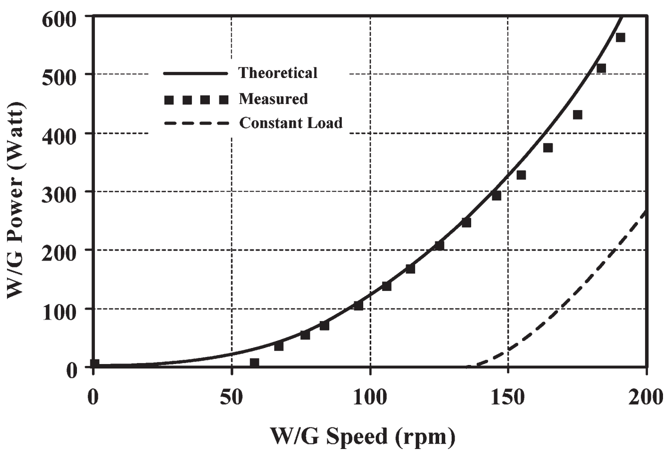

Fig. 11. WG theoretical and measured output power versus the rotor speed of rotation.

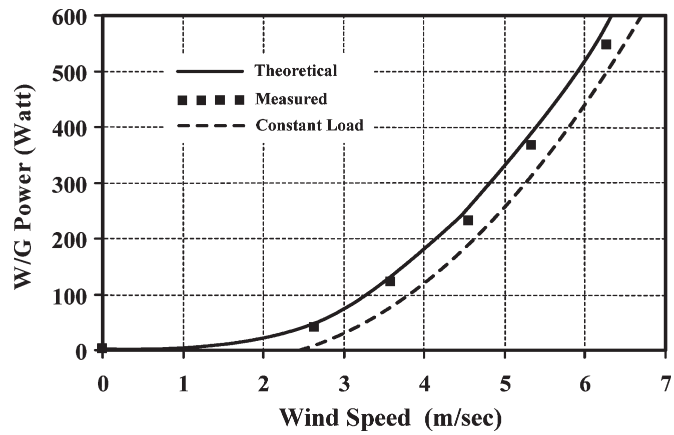

Fig. 12. WG theoretical and measured output power versus the wind speed.

the proposed MPPT method, the output power follows the optimal power versus the rotational-speed characteristic. The maximum deviation from the optimal line is approximately 7%, mainly due to a lower number of measurements in the power range of 400–600 W, while a 30% of this deviation is attributed to the rectifier power loss. For comparison purposes, the output power of a WG directly connected to a 24-V battery through a rectifier is also indicated in the figure. The power produced in that case is much lower compared to that with the proposed MPPT method.

For a further investigation of the WG-output-power behavior at various wind-speed levels, the measured wind-speed range was divided in intervals each of 1-m/s width. The ensemble average (P_k, V_k) of the WG power and wind-speed measurements corresponding to each interval is calculated as follows:

$$P_k = \frac{1}{n_k} \sum_{p=1}^{n_k} P_{kp} \tag{22}$$

$$V_k = \frac{1}{n_k} \sum_{p=1}^{n_k} V_{kp} \tag{23}$$

where V_{kp} is the pth wind-speed point in the kth interval, P_{kp} is the pth power point in the kth interval, and n_k is the number of data sets in the kth interval.

The resulting ensemble averages (P_k, V_k) are used to build the diagram shown in Fig. 12. It is noticed that the WG output power follows the optimal WG power versus wind-speed characteristic with a maximum deviation of approximately 6.5%, while the rectifier power loss is responsible for 30% of this deviation. The power production of a WG directly connected to a battery-rectifier load is also indicated in the same figure. The WG-output-power benefit using the proposed MPPT method, compared to the battery-rectifier configuration, is 11%–50% in the power range of 100–600 W. It is clearly concluded that the proposed method results in a better exploitation of the available wind energy, especially in the low wind-speed range of 2.5–4.5 m/s.

The power transferred to the battery bank is derived considering the dc/dc converter efficiency, the WG output power, and the rectifier power loss. The use of the proposed method improves the power transferred to the battery by 7%–45% in the power range of 100–600 W, compared to the simple battery-rectifier configuration.

The experimental results of the past-proposed WG MPPT methods either have been obtained with laboratory-built WG simulators, thus the MPPT performance under real conditions has not been exhibited, or their performance has not been adequately investigated so as to indicate the deviation from the optimal power production.

V. Conclusion

In this paper, the development of a novel WG maximum power tracking control system is presented, comprising of a high-efficiency buck-type dc/dc converter and a microcontroller-based control unit. The advantages of the proposed MPPT method are as follows: 1) no knowledge of the WG optimal power characteristic or measurement of the wind speed is required and 2) the WG operates at variable speed and thus suffering lower stress on the shafts and gears compared to constant-speed systems. The proposed MPPT method does not depend on the WG wind and rotor-speed ratings nor the dc/dc converter power rating.

Experimental results of the proposed system indicate that the WG output power is increased by 11%–50%, compared to the case where the WG is directly connected via a rectifier to the battery bank. The proposed method results in a better exploitation of the available wind energy, especially in the low wind-speed range of 2.5–4.5 m/s, where the power production of the battery-rectifier configuration is relatively low.

The proposed method can be easily extended to include battery charging management or additional RES control, while it can also be modified to control a dc/ac converter in the case of a grid-connected wind-energy-conversion system.

References

[1] N. Kodama, T. Matsuzaka, and N. Inomata, "Power variation control of a wind turbine generator using probabilistic optimal control, including feed-forward control from wind speed," *Wind Eng.*, vol. 24, no. 1, pp. 13–23, Jan. 2000.

[2] L. L. Freris, *Wind Energy Conversion Systems*. Englewood Cliffs, NJ: Prentice-Hall, 1990, pp. 182–184.

[3] V. Valtchev, A. Bossche, J. Ghijselen, and J. Melkebeek, "Autonomous renewable energy conversion system," *Renew. Energy*, vol. 19, no. 1, pp. 259–275, Jan. 2000.

[4] E. Muljadi and C. P. Butterfield, "Pitch-controlled variable-speed wind turbine generation," *IEEE Trans. Ind. Appl.*, vol. 37, no. 1, pp. 240–246, Jan. 2001.

[5] A. M. De Broe, S. Drouilhet, and V. Gevorgian, "A peak power tracker for small wind turbines in battery charging applications," *IEEE Trans. Energy Convers.*, vol. 14, no. 4, pp. 1630–1635, Dec. 1999.

[6] O. Honorati, G. Lo Bianco, F. Mezzetti, and L. Solero, "Power electronic interface for combined wind/PV isolated generating systems," in *Proc. Eur. Union Wind Energy Conf.*, Göteborg, Sweden, 1996, pp. 321–324.

[7] G. Lo Bianco, O. Honorati, and F. Mezzetti, "Small-size stand alone wind energy conversion system for battery-charging," in *Proc. 31st Universities Power Engineering Conf.*, Iráklion, Greece, 1996, pp. 62–65.

[8] R. Spee, S. Bhowmik, and J. Enslin, "Novel control strategies for variable-speed doubly fed wind power generation systems," *Renew. Energy*, vol. 6, no. 8, pp. 907–915, Nov. 1995.

[9] A. Z. Mohamed, M. N. Eskander, and F. A. Ghali, "Fuzzy logic control based maximum power tracking of a wind energy system," *Renew. Energy*, vol. 23, no. 2, pp. 235–245, Jun. 2001.

[10] R. M. Hilloowala and A. M. Sharaf, "A rule-based fuzzy logic controller for a PWM inverter in a stand alone wind energy conversion scheme," *IEEE Trans. Ind. Appl.*, vol. 32, no. 1, pp. 57–65, Jan./Feb. 1996.

[11] N. Mohan, T. Undeland, and W. Robbins, *Power Electronics: Converters, Applications and Design*, 2nd ed. New York: Wiley, 1995, pp. 164–172.

Eftichios Koutroulis was born in Chania, Crete, Greece, in 1973. He received the B.S., M.S. and the Ph.D. degrees in the area of power electronics and renewable energy sources (RES), in 1996, 1999, and 2002, respectively, from the Department of Electronic and Computer Engineering, Technical University of Crete, Chania, Greece.

He is currently a Research Associate in the Department of Electronic and Computer Engineering, Technical University of Crete. His research interests include photovoltaic and wind-energy-conversion systems, energy management systems with RES, power electronics (dc/ac inverters and dc/dc converters), data-acquisition systems, sensors and transducers, and microcontroller-based systems.

Kostas Kalaitzakis was born in Chania, Crete, Greece, in 1954. He received the B.S. degree in electrical and mechanical engineering from the National Technical University of Athens, Zographou, Greece, and the Ph.D. degree in renewable energy sources (RES) from the School of Electrical Engineering, Democritus University of Thrace, Xanthi, Greece, in 1977 and 1983, respectively.

He is currently a Professor at the Technical University of Crete, Chania, Greece. He served as an Adjunct Assistant Professor at the Georgia Institute of Technology, Atlanta. His current research interest include renewable energy sources, energy saving in buildings, power electronics, sensors and measurement systems, smart cards applications, fuzzy, neural, and genetic decision support and control systems, bioengineering, and local operating networks.